

TOLERANCES OF CRAB DISPERSION AT THE INTERACTION POINT IN THE HADRON STORAGE RING OF THE ELECTRON-ION COLLIDER*

Y. Luo[†], J. S. Berg, M. Blaskiewicz, C. Montag, V. Ptitsyn, F. Willeke, D. Xu
Brookhaven National Laboratory, Upton, NY, USA

Y. Hao, Facility for Rare Isotope Beams, Michigan State University, East Lansing, MI, USA

J. Qiang, Lawrence Berkeley National Laboratory, Berkeley, CA, USA

V. Morozov, Oak Ridge National Laboratory, Oak Ridge, TN, USA

T. Satogata, Thomas Jefferson National Accelerator Facility, Newport News, VI, USA

Abstract

The Electron Ion Collider (EIC) presently under construction at Brookhaven National Laboratory will collide polarized high energy electron beams with hadron beams with luminosities up to $1 \times 10^{34} \text{cm}^{-2} \text{s}^{-1}$ in the center mass energy range of 20-140 GeV. Due to the detector solenoid in the interaction region, the design horizontal crabbing angle will be coupled to the vertical plane if uncompensated. In this article, we study the tolerances of crab dispersion at the interaction point in the EIC Hadron Storage Ring (HSR). Both strong-strong and weak-strong simulations are used. We found that there is a tight tolerance of vertical crabbing angle at the interaction point in the HSR.

INTRODUCTION

The Electron Ion Collider (EIC) presently under construction at Brookhaven National Laboratory will collide polarized high energy electron beams with hadron beams with luminosities up to $1 \times 10^{34} \text{cm}^{-2} \text{s}^{-1}$ in center mass energy range of 20-140 GeV [1]. To reach such a high luminosity, we adopt high bunch intensities for both beams, small transverse beam sizes at the interaction point (IP), a large crossing angle 25 mrad, and a novel strong hadron cooling in the Hadron Storage Ring (HSR) at store energies. To compensate the geometric luminosity loss due to the large crossing angle, crab cavities are installed on both sides of IP to restore head-on collision.

Based on the operational experiences of previous and existing lepton and hadron colliders, we must have a very good control of optics parameters at IP to achieve the design luminosity and to maintain a stable physics store. Those parameters include orbit, Twiss parameters, momentum dispersion, local coupling, and so on. In the EIC, the horizontal crab cavities will create a z -dependent horizontal offset along the bunch length at IP. Here z is the longitudinal offset w.r.t. the bunch center. Conventionally, we define dx/dz as the horizontal crab dispersion. There are other three terms of first order crab dispersion: dx'/dz , dy/dz , dy'/dz . dy/dz is the vertical crab dispersion. In this article, we also call dx/dz and dy/dz at IP as horizontal and vertical crabbing angles.

We adopt a local crabbing compensation scheme for the EIC. We need to have $dx/dz = 12.5 \times 10^{-3}$ at IP and to keep other 3 first order crab dispersion to be zero or close to zero as possible. However, due to the detector solenoid in the interaction region (IR), horizontal crab dispersion may be coupled to the vertical plane and generate non-zero vertical crab dispersion at IP. To avoid vertical orbit excursions at the non-collisional symmetric points in IRs, we intentionally tilt the Electron Storage Ring (ESR) by 200 μrad with the axis connecting IP6 and IP8. Therefore, the ESR and HSR will not be in a same horizontal plane anymore. This generates an equivalent vertical crabbing angle 50 μrad at IP for both rings. Other coupling sources, such as residual magnet roll errors, vertical orbit in sextupoles, and crab cavity roll error, also can couple horizontal crab dispersion to vertical plane.

Vertical crab dispersion or vertical crabbing angle at IP will generate a z -dependent vertical offset along the bunch length. Offset beam-beam interaction may cause the proton beam emittance blow up and leads to a bad proton beam life. In this article, we will study the tolerances of crab dispersion at IP, in particular, we will focus on the vertical crab dispersion dy/dz . The design beam and machine parameters for the collision between polarized 10 GeV electrons and 275 GeV protons are used. At this mode, the design transverse beam sizes at IP are (95 μm , 8.5 μm). Both beams reach their maximum beam-beam parameters in the EIC, that is, 0.1 for the electron beam and 0.015 for the proton beam [2]. The design peak luminosity is $1.0 \times 10^{34} \text{cm}^{-2} \text{s}^{-1}$.

STRONG-STRONG SIMULATION

Two kinds of beam-beam simulation models have been used for the EIC: strong-strong and weak-strong [3–5]. In the strong-strong model, both beams are represented by a half to 2 millions of macro-particles. At IP, each bunch is longitudinally sliced. Each slice of one bunch will interact with all slices from the opposite bunch in a timed order. The space charge or beam-beam force is calculated with Particle-in-cell (PIC) Poisson solver. The ring lattice is simply represented by a linear uncoupled 6×6 matrix. Synchrotron motion is included.

In our simulation, the horizontal crab cavities are virtually placed on both sides IP with an exact $\pi/2$ horizontal betatron phase advances to IP. This arrangement constructs a closed local horizontal crab dispersion bump. To introduce a vertical crab dispersion dy/dz at IP, similarly we place a vertical

* Work supported by Brookhaven Science Associates, LLC under Contract No. DE-SC0012704 with the U.S. Department of Energy.

[†] yluo@bnl.gov

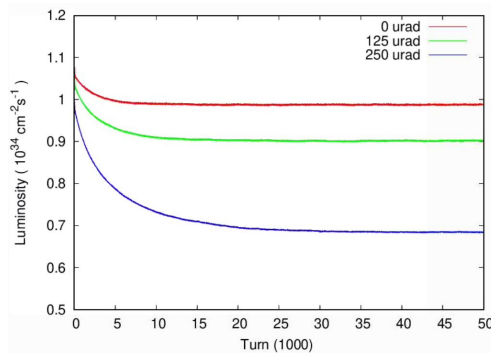


Figure 1: Luminosity evolution with three vertical crab dispersion at IP. Strong-strong model is used.

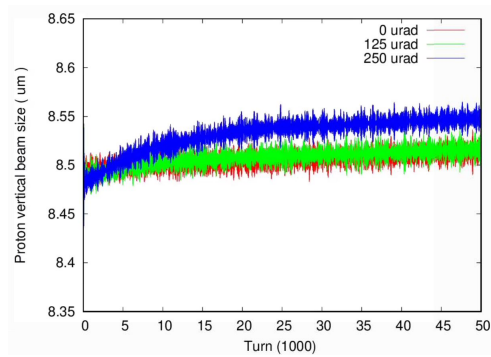


Figure 2: Proton vertical beam sizes with three vertical crab dispersion at IP. Strong-strong model is used.

crab cavity on either side of IP with an exact vertical phase advance $\pi/2$ to IP. By adjusting their voltages, we are able to scan dy/dz at IP while with no net contribution to dx/dz , dx'/dz , and dy'/dz at IP.

Figure 1 shows the luminosity evolution over 50,000 turns with 3 settings of vertical crab dispersion at IP. From the plot, after the early 20,000 turns of transient period due to synchrotron radiation effects in the ESR, the so-called equilibrium state is reached. From the plot, the equilibrium luminosity drops 30% and 8% with vertical crab dispersion 250 μrad and 150 μrad at IP, compared to the ideal case without vertical crab dispersion.

We paid a lot of attention to the stability of proton beam with beam-beam interaction, especially in the vertical plane. Figure 2 shows the evolution of the proton bunch's vertical beam size in 50,000 turns. From the plot, the proton vertical beam growth with 250 μrad vertical crab dispersion at IP is visible and faster than that with 125 μrad and zero vertical crab dispersion at IP.

Strong-strong beam-beam simulation is subject to numerical noises. The simulated growth rates of proton beam sizes are largely affected by the numbers of macro-particles, transverse grids, and longitudinal slices. For cross-check, we normally will carry out weak-strong simulations following strong-strong simulations.

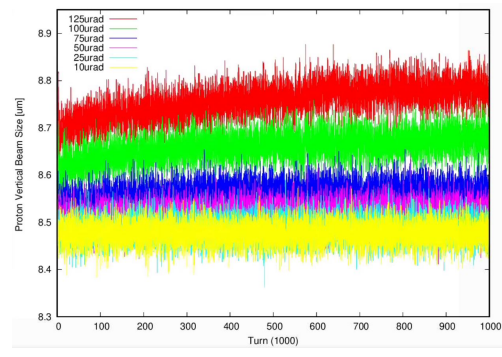


Figure 3: Vertical beam size evolution with different vertical crab dispersion at IP. Weak-strong model is used.

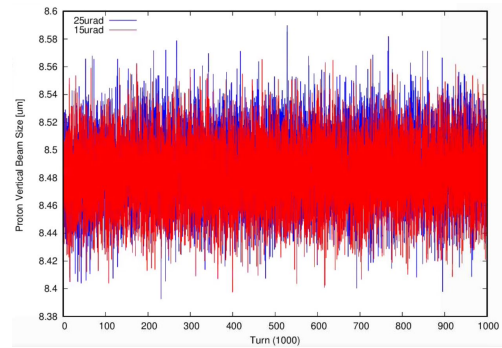


Figure 4: Vertical beam size evolution with vertical crab dispersion 15 μrad and 25 μrad at IP. Weak-strong model is used.

WEAK-STRONG SIMULATION

In the weak-strong beam-beam simulation model, the proton bunch is still represented by macro-particles but the electron bunch is represented with a rigid 6-d Gaussian charge distribution. The beam-beam force is analytically calculated with the Bassetti-Erskine formula. Compared to strong-strong model, weak-strong model has much less numerical noise. However, it is not self-consistent since it assumes that the strong bunch is not affected by the weak bunch. Weak-strong model is valid when there is no coherent beam-beam instability, which is true for the EIC.

In this study, we use 30,000 macro-particles for the proton bunch to save the computing time. They are tracked up to 1 million turns. We calculate the proton bunch's geometric RMS beam sizes every turn. After tracking, we fit the proton beam sizes between 0.5 to 1 million turns with a linear function and extrapolate the slope to a relative beam size growth rate $d\sigma/dt/\sigma$ in a unit of %/hour.

Figure 3 shows the simulated proton vertical beam size evolution with different vertical crab dispersion at IP. From the plot, vertical crab dispersion at IP more than 50 μrad will have a clear faster growth rate than the case without vertical crab dispersion.

Table 1 lists the simulated proton beam size growth rates for various settings of vertical crab dispersion at IP. From it, the vertical proton beam size growth rate is less than

Table 1: Simulated Proton Vertical Beam Size Growth Rate Versus Vertical Crab Dispersion at IP

dy/dz at IP (μrad)	Horizontal beam size growth rate (%/h)	Vertical beam size growth rate (%/h)
0	-0.4	-0.8
5	0.6	0.2
10	0.9	-3.9
15	-1.0	17.1
20	-0.1	-2.4
25	-0.4	-2.8
30	-3.6	23.3
40	-1.5	13.4
50	3.0	31.0
75	0.5	12.7
100	0.6	79.3
125	-4.2	100.1

10%/hour when vertical crab dispersion is less than 25 μrad , except with one case with 15 μrad vertical crab dispersion at IP. In this study, we found it is difficult to have a very accurate growth rate calculation below 20%/hour. For example, Figure 4 shows the proton beam size evolution with vertical crab dispersion 15 μrad and 25 μrad at IP. It is hard to tell their difference visibly.

Based on the above weak-strong simulation results, we set the tolerance of vertical crab dispersion at IP to be 25 μrad , which is only 0.4% of the design horizontal crab dispersion at IP.

DYNAMIC APERTURE CALCULATION

Next we calculate proton beam's dynamic aperture with vertical crab dispersion at IP with SimTrack [5]. For the latest HSR lattice, the horizontal phase advance between two side crab cavities is 5 degrees off 180 degrees so that the IR horizontal crab dispersion is not closed. To have a clean study with vertical crab dispersion at IP, we insert artificial phase trombones in IR to make the horizontal phase advance between IP and crab cavities to be exact 90 degrees and there is no horizontal crab dispersion leakage into the arcs. For simplicity, we simply apply vertical crab cavity kicks at IP to introduce vertical crab dispersion at IP, in the same way we did in the above strong-strong and weak-strong simulations.

For a quick estimate, we first only calculate the minimum dynamic aperture in the 15 degree direction in the phase space ($x/\sigma_x, y/\sigma_y$). For a flat beam in the HSR, the minimum dynamic aperture normally happens in a lower phase angle. Table 2 shows the calculated 10^6 turn dynamic aperture in a vertical crab dispersion scan. For each vertical crab dispersion setting, we track with 10 seeds of IR nonlinear magnetic field errors. We list the minimum, maximum, and average dynamic apertures for each dy/dz setting.

From Table 2, if we assume that the acceptable minimum dynamic aperture should be higher than 5σ to guarantee a sufficient proton lifetime, then the tolerance of vertical crab dispersion at IP will be about 20 μrad .

Table 2: Dynamic Aperture Versus Vertical Crab Dispersion at IP

dy/dz at IP (μrad)	DA-Min (σ)	DA-Max (σ)	DA-Ave (σ)	DA-RMS (σ)
0	6.2	10.2	8.0	1.2
5	6.2	9.8	7.5	1.0
10	5.6	10.8	8.2	1.4
20	5.2	11.6	7.8	1.9
30	5.6	10.4	8.0	1.4
40	4.8	11.4	7.8	1.8
50	5.8	10.4	7.9	1.1
60	4.8	8.6	6.7	1.3

DISCUSSIONS

We also studied the tolerances for dx'/dz and dy'/dz at IP with strong-strong and weak-strong simulation models. The tolerance for dx'/dz at IP is found about $1 \times 10^{-4} \text{m}^{-1}$, while the tolerance for dy'/dz at IP about $1 \times 10^{-5} \text{m}^{-1}$. The reason for a smaller tolerance for dy'/dz than dx'/dz at IP is probably related to the flat beams at IP in the EIC. In the above tolerance simulation studies, we assumed there was only one kind of crab dispersion errors among the four linear crab dispersion terms. If with combined dy/dz , dx'/dz , and dy'/dz at IP, the crab dispersion tolerances are expected to be even tighter.

We also estimated the residual crab dispersion at IP due to alignment roll errors of magnets and crab cavities. With current HSR lattice, if we do not correct the horizontal crab dispersion leakage in the ring due to the unclosed horizontal crab dispersion in IR6, we will have vertical crab dispersion about 1 μrad at IP with a random RMS roll error 100 μrad to all quadrupoles in the HSR. With a closed horizontal crab dispersion bump, if all crab cavities on one side of IP are accidentally tilted by 200 μrad , the residual vertical crab dispersion at IP is about 0.2 μrad .

In the future EIC operation, we need to have a robust algorithm and a reliable online system to compensate the residual vertical crab dispersion at IP. We planned to append skew quadrupole wires to IR quadrupoles close to IP to compensate the effects from the detector solenoid and ESR tilting. These skew quadrupole correctors may also be used for residual vertical crab dispersion correction at IP. Further design and simulation studies are in progress.

CONCLUSION

In this article, we studied the tolerances of vertical crab dispersion at the interaction point in the Hadron Storage Ring of the EIC. Strong-strong, weak-strong beam-beam simulations, together with dynamic aperture calculation are carried out for this purpose. Based on the simulation results with weak-strong mode and quick dynamic aperture calculation, the vertical crab dispersion tolerance at IP is about 20-25 μrad , which requires an accurate and robust online correction system in the future EIC operation.

REFERENCES

- [1] C. Montag *et al.*, “Design Status Update of the Electron-Ion Collider”, in *Proc. IPAC’21*, Campinas, Brazil, May 2021, pp. 2585–2588. doi:10.18429/JACoW-IPAC2021-WEPAB005
- [2] Y. Luo *et al.*, “Beam-Beam Related Design Parameter Optimization for the Electron-Ion Collider”, in *Proc. IPAC’21*, Campinas, Brazil, May 2021, pp. 3808–3811. doi:10.18429/JACoW-IPAC2021-THPAB028
- [3] K. Ohmi “Simulation of beam-beam effects in a circular e^+e^- collider”, *Phys. Rev. E*, vol. 62, pp. 7287–7294, Nov. 2000. doi:10.1103/PhysRevE.62.7287
- [4] J. Qiang *et al.*, “A parallel particle-in-cell model for beam-beam interaction in high energy ring colliders”, *J. Comput. Phys.*, vol. 198, pp. 278–294, 2004. doi:10.1016/j.jcp.2004.01.008
- [5] Y. Luo “SimTrack: A compact c++ code for particle orbit and spin tracking in accelerators”, *Nucl. Instrum. Methods Phys. Res., Sect. A*, vol. 801, pp. 95-103, 2015. doi:10.1016/j.nima.2015.08.014